



Non-linear behavior of the transfer impedance of a Micro-Slit-Plate: effect of slit length in presence of a bias flow

Alessia Aulitto¹, Vertika Saxena, Avraham Hirschberg, Ines Lopez Arteaga
Eindhoven University of Technology
P.O. Box 513, 5600 MB Eindhoven, The Netherlands

ABSTRACT

The influence of the slit length in presence of bias flow for a micro-slit plate (MSP) is investigated. MSPs are plates with arrays of slit-shaped perforations, with width of the order of the acoustic viscous boundary layer thickness. Micro-slit plates can be used for passive noise control of thermo-acoustic instabilities in combustion processes. During these processes, high amplitudes acoustic waves are generated and impact on the plates. The geometry discussed in this work is typical for manufacturing by cutting and bending the plate, without removing material. In previous works, in presence of high acoustic amplitudes, a significant difference between short and long slits was observed. In this work, the influence of a bias flow is investigated. This bias flow can also be used to control the wall temperature in hostile environment or for air-conditioning. Impedance tube measurements of the transfer impedance on accurately manufactured micro-slit plates in presence of bias flow have been performed. It appears that the presence of flow does not reduce the effect of the slit length on the transfer impedance of the micro-slit plate at high acoustic amplitudes.

1. INTRODUCTION

Micro-slit absorbers and plates (MSAs, MSPs) have been proposed as sound absorbers at low frequencies, providing lightweight and compact solutions to substitute conventional materials [1]. MSPs are plates with slit width b in the sub-millimeter range and low porosity (order of 1%). The slit width is of the order of the viscous-boundary-layer thickness δ_v . Hence, the ratio between the slit width and the viscous boundary layer thickness δ_v , the so-called Shear number $Sh = b/\delta_v$, is of order unity. In conventional designs, micro-slit plates are backed by a cavity forming micro-slit absorbers (MSAs) [1-3]. In many applications one can expect the presence of a main flow along the perforated wall or a bias flow through this wall. This is for instance the case in combustion chambers where bias flow is used to cool the wall. In Aulitto *et al.* the linear and non-linear transfer impedance for a given design of a micro-slit plate is investigated in the absence of flow [4]. The effect of the slit length is discussed. In the present work, the effect of the slit length is investigated in presence of bias flow for a given (high) acoustic excitation. Impedance tube measurements are used to investigate the effect of the slit length by comparison of results for two accurately manufactured micro-slit plates. The edges of the slits are kept as sharp as possible. Both plates have the same porosity and total slit perforation length.

The behavior of slits in presence of a grazing flow is studied in several publications. Systematic measurements in the linear regime are provided for grazing flow by Kooijman *et al.* and for combined grazing/bias flow by Tonon *et al.* and Moers *et al.* [5-6-7]. Tam *et al.* perform numerical simulations of the flow field around a slit resonator in the presence of a grazing flow under acoustic forcing [8]. Dai *et al.* propose a numerical study of the acoustical response of a slit with a mean bias flow by

¹ a.aulitto@tue.nl



means of a potential flow model [9]. Vandemaele *et al.* consider the linear, flow acoustic behavior of a slit resonator, mounted at the side of a flow duct, under grazing acoustic excitation [10]. Several publications investigate the effect of a bias flow for circular perforations and micro-perforated plates [11-17]. The present paper is structured as follows. In Section 2, the main parameters and dimensionless numbers are presented. In Section 3, the experimental setup and the geometrical properties of the samples are described. In Section 4, results of impedance tube measurements for a given amplitude are presented for different bias flow velocities. In the last section, conclusions are summarized.

2. DEFINITIONS OF MAIN PARAMETERS

In the linear regime, dissipation of acoustic energy takes place in the oscillating boundary layer of thickness $\delta_v = \sqrt{2\mu/\omega\rho}$, where $\omega = 2\pi f$ is the angular frequency, ρ is the air density ($\rho = 1.18 \text{ kg/m}^3$ at 25° and atmospheric pressure) and μ is the dynamic viscosity of air ($\mu = 1.85 \times 10^{-5} \text{ kg/ms}$ at 25°). The ratio between the slit width b and the thickness of the viscous boundary layer δ_v is the Shear number

$$\text{Sh} = \frac{b}{\delta_v}. \quad (1)$$

For micro-slit plates, typical Shear numbers, in the frequency range of interest, are of order unity. The behavior of the plate can be studied as a function of the Strouhal number St , defined as the ratio between the slit width b and the amplitude of the oscillating particle displacement in the slits. In formulas,

$$\text{St} = \frac{\omega b}{U_p}, \quad (2)$$

where U_p is the cross-sectional surface averaged flow velocity at the slit. The concept of transfer impedance is introduced in the frequency domain (for purely harmonic oscillations of frequency f). The transfer impedance of the plate is defined as the ratio between the complex acoustic pressure difference $\Delta\hat{p}$ and the amplitude of the acoustical velocity \hat{u} in a pipe cross-section upstream from the plate. The dimensionless transfer impedance of the plate is

$$z_{\text{plate}} = \frac{\Delta\hat{p}}{\rho c \hat{u}}, \quad (3)$$

where ρ is the density of air and c is the speed of sound in air. The dimensionless transfer impedance of the plate z_{plate} is a complex quantity

$$z_{\text{plate}} = \text{Real}[z_{\text{plate}}] + \text{Imag}[z_{\text{plate}}], \quad (4)$$

with $i^2 = -1$, $\text{Real}[z_{\text{plate}}]$ the resistive part of the transfer impedance of the plate (or resistance of the plate) and $\text{Imag}[z_{\text{plate}}]$ the reactive part of the transfer impedance of the plate (or inertance of the plate). The transfer impedance of a slit is defined as the ratio between the complex pressure difference $\Delta\hat{p}$ and the amplitude of the cross-sectional acoustical velocity \hat{u}_p in the slit. In formulas,

$$z_{\text{slit}} = \frac{\Delta\hat{p}}{\rho c \hat{u}_p} = z_{\text{plate}} \Phi \quad (5)$$

where $\hat{u}_p = \hat{u}/\Phi$ and Φ the porosity of the plate. Therefore, in the first order of approximation the transfer impedance of the plate can be obtained from the impedance of a single slit [3]. The slit impedance will however slightly depend on the porosity, because of confinement effects and interaction between slits.

3. EXPERIMENTAL SETUP

A detailed description of the impedance tube setup and of the calculations for the transfer impedance of the samples can be found in (3). For the tests described in this work a Bronkhorst F-202AV meter is used to control the flow. Air is used. Tests are performed between $f = 20$ Hz and $f = 220$ Hz. One acoustic excitation equivalent to 10 Pa measured at the reference microphone (the one closer to the sample) is considered. The average flow velocity in the slits is varied from 0m/s to 3 m/s. Furthermore, a manometer (Anemometer TA400 Pitotbuis, 1 Pa accuracy) is used in the setup to measure the static pressure drop as function of the flow speed in absence of acoustic excitation. This is used to characterize the samples and investigate their difference for higher flow speeds than the one considered for this study. The samples discussed in this work are show in Figure 1 and Figure 2. The samples are accurately (few micrometers accuracy), milled in a 5mm thick brass plate. Sketches of the dimensions and main parameters are shown in Figure 3.



Figure 1 Sample with short slits



Figure 2 Sample with long slits

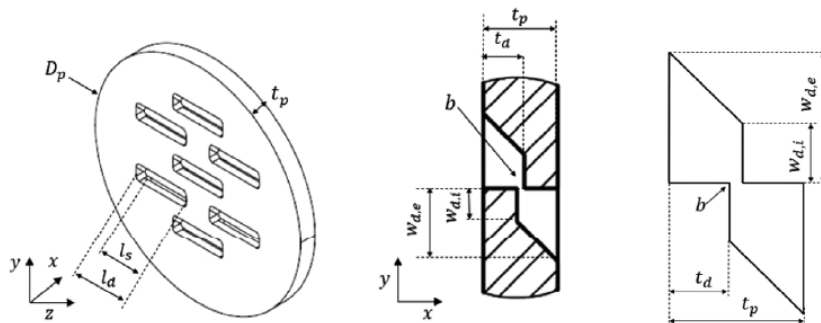


Figure 3 Sketches of the plate and of the cross-section of a single slit with parameters

The effective diameter of the portion of the plate where the slits are located $D_i = 50$ mm, with the internal diameter of the impedance tube. The total plate thickness is $t_p = 5$ mm and the nominal slit width is $b = 0.5$ mm. The external width of the ditch is $w_{d,e} = 5$ mm, the internal width of the ditch is $w_{d,i} = 2.25$ mm. The ditch thickness is $t_d = 2.75$ mm. The thickness of the plate at the slit is $t = t_p - t_d = 2.25$ mm. The slit length is $l_{s,short} = 15$ mm for short slits and $l_{s,long} = 35$ mm for long slits. The angle between the internal ditch and the outside ditch is 45° . The plates are realized in such

a way that the total length of the slits P is the same. The total slit length is $P = 7 \times l_{s,short} = 3 \times l_{s,long} \approx 105\text{mm}$. The porosity (of the portion of the plate in the impedance tube) is $\Phi = 2.7\%$. To provide access to the rotary cutter, the ditch length is longer than the slit length, $l_d = l_s + 2\text{mm}$.

4. RESULTS

3.1. Static pressure-drop results

In this subsection, the measured static pressure drop for short and long slits is presented as function of the flow velocity in the slits. Results of the static pressure difference Δp_0 presented in the form of a discharge coefficient pressure $\alpha = Q / (bl_s \sqrt{\frac{2\Delta p_0}{\rho}})$ where Q is the volume flux and l_s is the total length of the slits ($l_{s,short}$ for short slits and $l_{s,long}$ for long slits) and ρ is the density. Figure 4 shows the discharge coefficient as a function of the Reynolds number $Re = \frac{bU_p}{\nu} = \frac{Q}{l_s \nu}$. For $Re > 500$ the difference between long and short slits remains at most of the order of 2%. One can conclude that there is a not significant difference in the steady flow behavior between long and short slits. The black line in Figure 4 corresponds to the high Reynolds number limit predicted by Aulitto et al. [4].

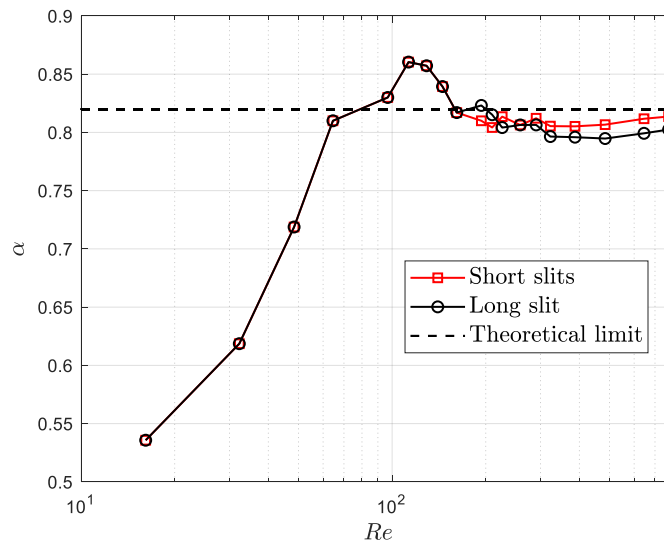


Figure 4 Static pressure drop as function of the flow speed in the slits

3.2. Acoustic measurements

In this subsection, results of the transfer impedance measurements for long and short slits are compared. In Figure 5, the real part the impedance of a slit is shown as function of the Shear number (frequency) for several flow speeds. The black lines in Figure 5 (and following) correspond to the plate with long slits, the red lines to the plate with short slits. It can be seen that the real part of the impedance increases for increasing flow speeds and the difference between long and short slits is maximum for the case of no flow (%) and reduces for increasing flow speeds. One observes a minor effect of the slit length and a poor collapse of data as a function of the Shear number. In Figure 6, the imaginary part of the impedance of a slit is shown as function of the Shear number. It can be seen that the imaginary part of the impedance increases with increasing frequency. In this case the effect of the slit length is more visible. In particular, the imaginary part of the impedance, or inertance, of short slits is 15% lower than the inertance of long slits due to the presence of 3D effects. Good

collapse of the data for different bias flows is observed for $Sh < 2.2$. Figure 7 and 8 show the real and imaginary part of the transfer impedance of a slit as function of the inverse of the Strouhal number of the flow for several flow speeds. Each of the curves corresponds to a different flow speed. One observes a fair collapse of data for the real part of the impedance as function of the Strouhal number of the flow and a large relative difference between the behavior without and with flow.

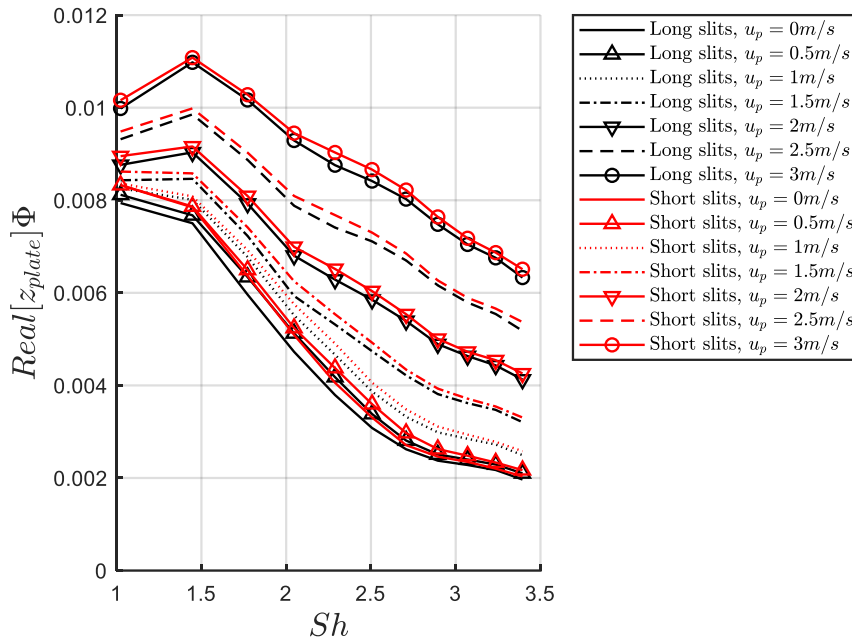


Figure 5 Real part of the impedance of a slit as function of the Shear number

4. CONCLUSIONS

In this work, experimental results obtained with an impedance tube show the effect of the slit length on the transfer impedance of a micro-slit plate in presence of a bias flow. Results are obtained for a fixed high acoustic excitation amplitude and for different flow speeds. Two accurately manufactured samples with sharp edges are considered for this study. While the discharge coefficient approaches for both long and short slits the potential flow limit for $Re > 500$, at lower Re a change of behavior with respect to higher Re is observed, that deserve further study. It appears that the behavior of the flow has a significant effect on the behavior of the transfer impedance. For increasing flow velocity, at a given high acoustic excitation amplitude, the real part of the transfer impedance of a slit increases while the imaginary part decreases. The real part of the impedance or resistance is marginally affected by the length of the slits. The imaginary part of the impedance or inertance of short slits is 15% lower than the case of long slits. This is similar to the behavior for the no-flow case discussed in Aulitto *et al.* [4].

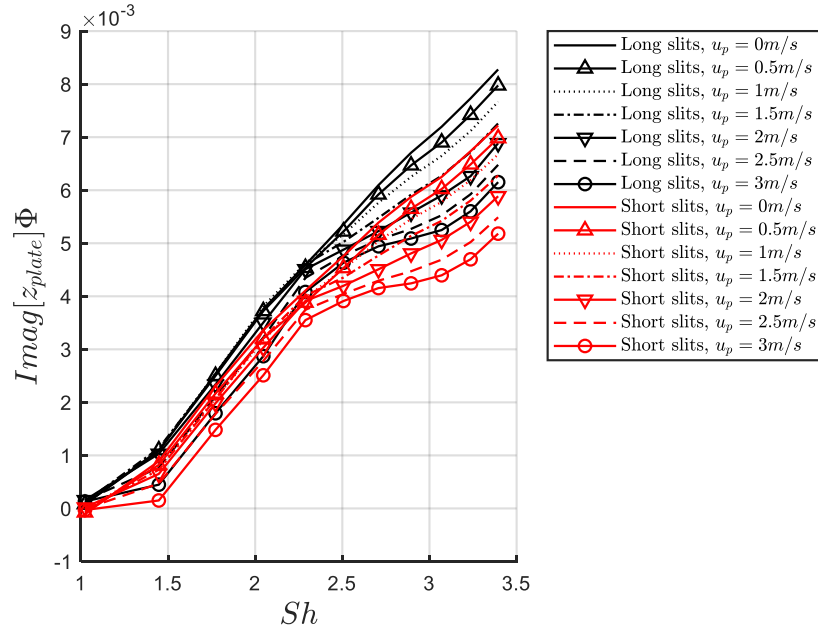


Figure 6 Imaginary part of the impedance of a slit as function of the Shear number

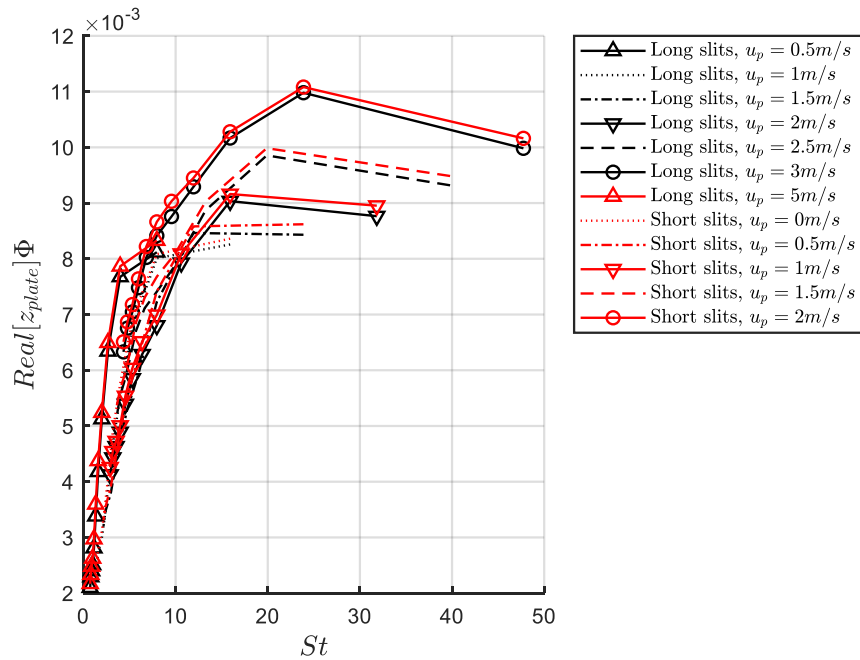


Figure 7 Real part of the impedance of a slit as function of the Strouhal number

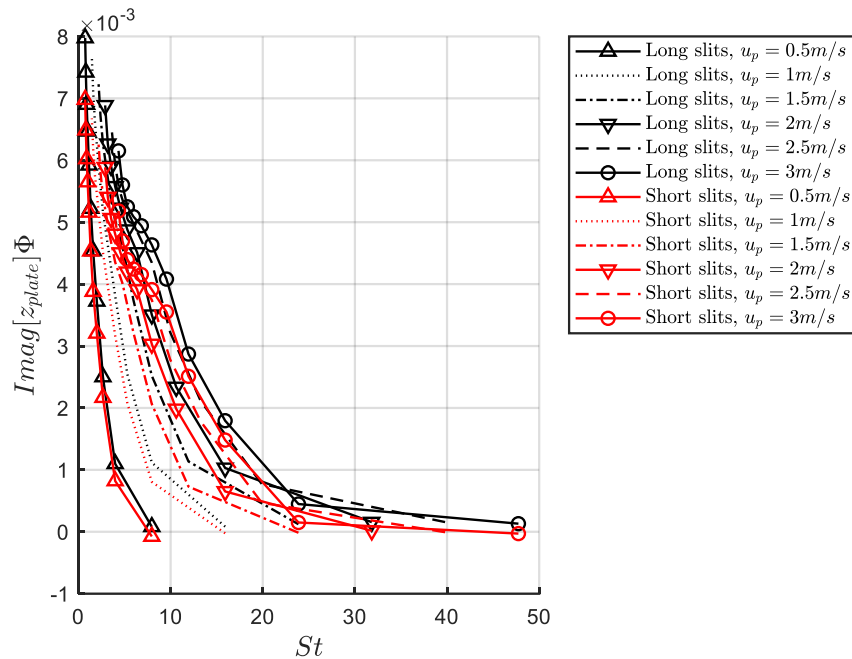


Figure 8 Imaginary part of the impedance of a slit as function of the Strouhal number.

5. ACKNOWLEDGEMENTS



This work is part of the Marie Skłodowska-Curie Initial Training Network Pollution Know-How and Abatement (POLKA). We gratefully acknowledge the financial support from the European Commission under call H2020-MSCA-ITN-2018 (project number: 813367).

REFERENCES

- [1] D. Maa, "Theory of microslit absorbers", *Chinese Journal of Acoustics*, 2000 .X. Jing and X. Sun, "Effect of Plate Thickness on Impedance of Perforated Plates with Bias Flow," vol. 38, no. 9, 2000.
- [2] R. T. Randeberg, "Adjustable slitted panel absorber," *Acta Acust. united with Acust.*, vol. 88, no. 4, pp. 507–512, 2002.
- [3] A. Aulitto, A. Hirschberg, and I. L. Arteaga, "Influence of geometry on acoustic end-corrections of slits in microslit absorbers", *JASA*, vol. 3073, 2021, doi: 10.1121/10.0004826.
- [4] A. Aulitto, A. Hirschberg, and I. L. Arteaga and E.L. "Effect of slit length on linear and non-linear acoustic transfer impedance of a micro-slit plate." *Acta Acustica*, 6, 6. <https://doi.org/10.1051/aacus/2021059>
- [5] D. Tonon, E. M. T. Moers, and A. Hirschberg, "Quasi-steady acoustic response of wall perforations subject to a grazing-bias flow combination," *J. Sound Vib.*, vol. 332, no. 7, pp. 1654–1673, 2013, doi: 10.1016/j.jsv.2012.11.024.
- [6] G. Kooijman, A. Hirschberg, and J. Golliard, "ARTICLE IN PRESS Acoustical response of



- orifices under grazing flow : Effect of boundary layer profile and edge geometry,” vol. 315, pp. 849–874, 2008, doi: 10.1016/j.jsv.2008.02.030.
- [7] E. M. T. Moers, D. Tonon, and A. Hirschberg, “Strouhal number dependency of the aero-acoustic response of wall perforations under combined grazing-bias flow,” *J. Sound Vib.*, vol. 389, pp. 292–308, 2017, doi: 10.1016/j.jsv.2016.11.028.
- [8] C. K. W. Tam, H. Ju, and B. E. Walker, “Numerical Simulation of a Slit Resonator in a Grazing Flow.”
- [9] Dai, X. Jing, and X. Sun, “Acoustic-excited vortex shedding and acoustic nonlinearity at a rectangular slit with bias flow,” *J. Sound Vib.*, vol. 333, pp. 2713–2727, 2014, doi: 10.1016/j.jsv.2014.02.029.
- [10] S. Vandemaele, H. Denayer, J. Tournadre, W. De Roeck, and W. Desmet, “Flow acoustic modeling of a slit resonator using linearized Navier-Stokes equations,” 2018.
- [11] D. Zhao, Y. Sun, S. Ni, C. Ji, and D. Sun, “Experimental and theoretical studies of aeroacoustics damping performance of a bias-flow perforated orifice,” *Appl. Acoust.*, vol. 145, pp. 328–338, 2019, doi: 10.1016/j.apacoust.2018.10.025.
- [12] S. Lee, J. Ih, and K. S. Peat, “ARTICLE IN PRESS A model of acoustic impedance of perforated plates with bias flow considering the interaction effect,” vol. 303, pp. 741–752, 2007, doi: 10.1016/j.jsv.2007.02.001.
- [13] D. This, “Sound absorption by perforated walls experimental study of the influence of geometry and bias / grazing flow Sound absorption by perforated walls,” 2011.
- [14] E. Moers, D. Tonon, and A. Hirschberg, “Sound absorption by perforated walls with bias / grazing flow : experimental study of the influence of perforation angle,” *Acoust. 2012, Société Française d’Acoustique*, pp. 3449–3453, 2012.
- [15] L. Zhou and H. Bodén, “Experimental investigation of an in-duct orifice with bias flow under medium and high level acoustic excitation,” pp. 267–292, 2014, doi: 10.1260/1756-8277.6.3.267.
- [16] X. Q. Ma and Z. T. Su, “Development of acoustic liner in aero engine: a review,” *Sci. China Technol. Sci.*, 2020, doi: 10.1007/s11431-019-1501-3.
- [17] J. Rupp, “Interaction Between the Acoustic Pressure Fluctuations and the Unsteady Flow Field Through,” vol. 132, no. June, pp. 1–9, 2010, doi: 10.1115/1.4000114.
- [18] D. Fabre, R. Longobardi, V. Citro, and P. Luchini, “Acoustic impedance and hydrodynamic instability of the flow through a circular aperture in a thick plate,” 2020, doi: 10.1017/jfm.2019.953.